INTERNATIONAL JOURNAL OF Experimental Pathology

*Int. J. Exp. Path.* (2015), 96, 151–162

ORIGINAL ARTICLE

# Oral administration of dextran sodium sulphate induces a caecum-localized colitis in rabbits

Irina Leonardi*, Flora Nicholls†, Kirstin Atrott*, Alexandra Cee*, Bernhard Tewes‡, Roland Greinwald‡, Gerhard Rogler* and Isabelle Frey-Wagner*

**Division of Gastroenterology and Hepatology, University Hospital Zurich, Zurich, Switzerland, †Central Biological Laboratory, University Hospital Zurich, Zurich, Switzerland and ‡Research and Development, Dr. Falk Pharma GmbH, Freiburg, Germany*

INTERNATIONAL JOURNAL OF EXPERIMENTAL PATHOLOGY

doi: 10.1111/iep.12117

Received for publication: 21 May 2014
Accepted for publication: 9 December 2014

**Correspondence:**
Isabelle Frey-Wagner
Klinik für Gastroenterologie und Hepatologie
Universitäts Spital Zürich
Raemistrasse 100
CH-8091 Zürich
Switzerland
Tel.: +41 (0)44 255 9916
Fax: +41 (0)44 255 9496
E-mail: isabelle.frey@usz.ch

## SUMMARY

*Trichuris suis ova* (TSO) have shown promising results in the treatment of inflammatory bowel disease (IBD) but the mechanisms which underlies this therapeutic effect cannot be studied in mice and rats as *T. suis* fails to colonize the rodent intestine, whilst hatching in humans and rabbits. As a suitable rabbit IBD model is currently not available, we developed a rabbit colitis model by administration of dextran sodium sulphate (DSS). White Himalayan rabbits ($n$ = 12) received 0.1% DSS in the daily water supply for five days. Clinical symptoms were monitored daily, and rabbits were sacrificed at different time points. A genomewide expression analysis was performed with RNA isolated from caecal lamina propria mononuclear cells (LPMC) and intestinal epithelial cells (IEC). The disease activity index of DSS rabbits increased up to 2.1 ± 0.4 ($n$ = 6) at day 10 (controls <0.5). DSS induced a caecum-localized pathology with crypt architectural distortion, stunted villous surface and inflammatory infiltrate in the lamina propria. The histopathology score reached a peak of 14.2 ± 4.9 ($n$ = 4) at day 10 (controls 7.7 ± 0.9, $n$ = 5). Expression profiling revealed an enrichment of IBD-related genes in both LPMC and IEC. Innate inflammatory response, Th17 signalling and chemotaxis were among the pathways affected significantly. We describe a reproducible and reliable rabbit model of DSS colitis. Localization of the inflammation in the caecum and its similarities to IBD make this model particularly suitable to study TSO therapy *in vivo*.

**Keywords**
Crohn's disease, DSS colitis, rabbit model of inflammatory bowel disease, RNA sequencing, *Trichuris suis*, ulcerative colitis

Inflammatory bowel diseases (IBD) can be regarded as a 'postindustrial revolution epidemic' as the frequency of these diseases has increased dramatically in the last 60 years (Molodecky *et al.* 2012). Initially, this increase was explained on the basis of the hygiene hypothesis that linked the improved hygienic conditions and the consequent reduction of childhood infections to an increase in the prevalence and incidence of immune-related diseases (Strachan 1989). Today it is assumed that the increase in hygiene standards reduces the interactions with micro-organisms that co-evolved with the immune system and influences the balance between immune-regulatory and effector mechanisms (Rook 2011).

In 2000, Elliot and colleagues focused their attention on the complementarity between the distribution of IBD and of helminth infections (Elliott *et al.* 2000; Weinstock *et al.* 2002). In their work they set the basis for the clinical application of a helminth therapy and proposed the whipworm parasite *Trichuris suis* as a therapeutic agent (Summers *et al.* 2003). Overall, the treatment with *T. suis* ova (TSO) proved to be safe with only mild and transient gastrointestinal effects reported (Scholmerich 2013). Those early results for efficacy in IBD were promising. However, two recent large multicenter trials in mild to moderate Crohn's disease with or without immunosuppression could not demonstrate a significant benefit of TSO treatment over placebo. Further clinical trials in ulcerative colitis are still under discussion. So far most studies have focused on the clinical efficacy and safety, and the mechanisms underlying the TSO treatment

effects remain unsolved. The discussion on whether further clinical studies should be undertaken (i.e. in ulcerative colitis) has given rise to a request for a better understanding of potential mechanisms and this implies establishment of suitable animal models.

Animal models of colitis are essential for the understanding of the aetiology and pathophysiology of IBD and constitute an essential tool in the development of new therapies. Currently, more than 66 different IBD models have been developed in several species including mouse, rat, rabbit and tamarin (Wirtz & Neurath 2000). Generally, IBD models can be subdivided into four categories of experimental colitis depending on the method of induction: congenital, genetically engineered, chemically induced and cell transfer induced (Mizoguchi 2012).

Most methods are used successfully in both mouse and rat. Unfortunately, research on the therapeutic application of *T. suis* in model organisms is complicated by the unsuccessful hatching of the ova in the mouse and rat intestine (unpublished data). In contrast, the life cycle of these parasites in the human and rabbit intestine is similar. In both hosts, *T. suis* hatch and establish in the distal intestine region where the larvae seem to die prematurely without reaching sexual maturity (unpublished data). Therefore, a colitis model in the rabbit would be a valuable tool to investigate the mechanisms underlying *T. suis* therapy.

Thus far the established rabbit IBD models have several drawbacks that limit their use for translational research. Rectal application of acetic acid causes severe acute inflammation, ischaemia and erosion within one day postapplication, but fails to induce chronic inflammation (Hathaway *et al.* 1999; Murthy 2006). Similarly, trinitrobenzene sulphonic acid (TNBS) dissolved in ethanol is also applied in the rectum. Within a week after application, TNBS induces a fully developed inflammation that presents ulcerative lesions and transmural inflammation (Anthony *et al.* 1995, 2007). However, the development of chronic inflammatory lesions in the TNBS model is highly variable and does not show good reproducibility (Knollmann *et al.* 2002). Furthermore, the short-term and self-limiting nature of these colitis models is not adequate for the study of the relapsing and remitting course of IBD. Both acetic acid and TNBS are introduced as an enema in the rabbit rectum and induce an inflammation that is usually confined to the distal colon, whereas *T. suis* ova hatch and develop in the ileum and caecum. Further colitis models in rabbits are of limited use either because of the complicated induction procedure (Hodgson *et al.* 1978; Hotta *et al.* 1986) or because of the high variability of the induced pathology (Watt & Marcus 1970).

Thus, a novel colitis model in the rabbit that allows the study of the mechanisms underlying the therapeutic effects of TSO treatment is needed.

In both mice and rats experimental colitis is commonly induced by the heparin-like polysaccharide dextran sodium sulphate (DSS). DSS increases the trans-epithelial permeability by decreasing the expression and by inducing the redistribution of tight junction proteins (occludin, zonula occludens-1, claudins) and by enhancing epithelial cell apoptosis (Poritz *et al.* 2007), (Yan *et al.* 2009), (Mennigen *et al.* 2009). Furthermore, DSS causes a hyperosmotic stimulus that leads to the activation of NF-κB in the epithelium (Schwartz *et al.* 2008). This is consistent with the accepted role of epithelial barrier dysfunction in the pathogenesis of IBD (Clayburgh *et al.* 2004). In both IBD and DSS colitis, the damaged epithelium allows the entry of luminal content into the mucosa, thereby facilitating the onset of inflammatory processes (Nell *et al.* 2010). In mice short-term administration of DSS (1–10% w/v) in drinking water is used to induce 'acute' colitis, whereas long-term or cyclic administration produces chronic colitis (Wirtz *et al.* 2007). The development of pathology can be easily monitored based on body weight, stool appearance, rectal bleeding and behavioural changes. Such clinical changes are usually preceded by alterations in histopathological parameters including colon shortening, mucosal injury, immune infiltration and epithelial damage. These changes initially appear in focal regions of the distal colonic mucosa and then expand progressively although the inflammation remains confined to the colon (Melgar *et al.* 2005).

The DSS model guarantees low risk of mortality, high reproducibility and good uniformity of the induced mucosal inflammation (Melgar *et al.* 2008). We therefore chose to develop a DSS colitis model in the rabbit. We found that in rabbits administration of 0.1% DSS for 5 days induces a clear caecum-localized inflammation that mimics histological features of ulcerative colitis and is characterized by a similar gene expression profile as observed in biopsies from patients with IBD. Furthermore, we describe a scoring system to correlate clinical parameters with histopathological findings that should facilitate the evaluation of the tested therapeutic approach.

## Methods

### *Rabbits*

All animal experiments were carried out according to Swiss animal welfare laws and approved by the veterinary office of Zurich. Female white Himalayan rabbits and New Zealand white rabbits (Charles River, Kisslegg, Germany) weighing 1.9–2.1 kg were used for the experiments. Rabbits were maintained single-housed with water and food (standard rabbit maintenance diet – Provimi Kliba AG, CH-4303 Kaiseraugst, hay and straw) *ad libitum* on a 12:12 h light/dark cycle. Upon arrival, animals were kept for at least four days under routine husbandry. One week prior to DSS exposure, drinking water was substituted by organic fennel tea (Hipp, Pfaffenhofen, Germany) *ad libitum*.

### Colitis induction and clinical evaluation

Colitis was induced by DSS (MP Biomedicals, Illkirch, France) dissolved in cold fennel tea at 0.1% w/v (if not specified otherwise). Control rabbits received fennel tea as vehicle. The beverage was prepared freshly and changed at least every second day. For every animal daily weight, daily food and fluid intake, daily stool appearance and behaviour were monitored. A disease activity index was calculated according to Table 1. The disease activity (range: 0–4) index represents the sum of individual scores for weight loss, presence of uneaten cecotrophs, food intake and beverage intake divided by 4. Euthanasia was performed following sedation with barbiturates with an overdose of ketamine hydrochloride (Vétoquinol, Bern, Switzerland) and xylazine (Bayer, Lyssach, Switzerland).

The abdominal cavity was exposed by a midline laparotomy, and samples were collected from the ileum, jejunum, duodenum, caecum and colon. For RNA extraction and myeloperoxidase activity analysis, the excised samples (0.5 cm in length) from the duodenum, jejunum, ileum and colon were opened by a longitudinal incision and rinsed with cold PBS. 1 $cm^2$ sections of the caecum were washed extensively with cold PBS until removal of the luminal content was complete. The samples were immediately snap-frozen in liquid nitrogen and stored at −80°C until analysis. For histological analysis samples (0.5 $cm^2$ sections of the caecum samples or 0.5 cm length sections of the other tissues) were either cut longitudinally or cut into smaller (0.2 cm) sections for fixation. The samples were carefully washed and fixed with phosphate-buffered 10% formalin solution. For genomewide mRNA expression studies, caecal samples (2 $cm^2$) were washed extensively with cold PBS and stored on ice in 5% BSA in PBS until further processing.

### Whole caecal tissue RNA extraction and quantitative real-time RT-PCR (qPCR)

Total RNA was isolated using the RNeasy Mini Kit (Qiagen, Hilden, Germany) and the automated sample preparation system Qiacube (Qiagen) following the manufacturer's recommendations. cDNA was synthesized with the High-capacity cDNA Reverse Transcription Kit (Life Technologies, Carlsbad, California, USA).

To study the transcription of immune response markers in rabbit intestine tissues, sequence-specific primers were applied (Table 2) and qPCR was performed according to Schnupf *et al.* with some modifications (Schnupf & Sansonetti 2012). Amplifications were performed in a total volume of 15 µl including 50 ng of cDNA, primers (0.2 µM each) and 7.5 µl of Power SYBR Green mix (Life Technologies). Reactions were run in triplicate on an ABI 7900HT (Life Technologies) using the universal thermal cycling parameters (2 min 54°C, 94.5°C 10 min, 40 cycles of 15 s at 97°C and 60 s at 59.7°C; dissociation curve: 15 s at 95°C, 15 s at 60°C and 15 s at 95°C). Results were analysed with the sequence detection software ABI 7900HT SDS2.4. For quality control purposes, all samples' dissociation curves were acquired and amplification products were visualized by 2% agarose gel electrophoresis. Primer sequences are listed in Table 2. The comparative $\Delta\Delta C_t$ method was applied for relative gene expression quantification ($C_t$: threshold cycle).

### Isolation of caecal lamina propria mononuclear cells (LPMC) and intestinal epithelial cells (IEC)

Caecal LPMC and IEC were isolated as previously described (Weigmann *et al.* 2007), with some

**Table 1** Scoring system for the daily monitoring of the disease activity index

| Score | Weight loss | Stool appearance and cecotrophs | Reduction in food intake | Reduction in beverage intake | Fur appearance |
|---|---|---|---|---|---|
| 0 | None | Well-formed solid pellets, 0 cecotrophs | None | None | Clean, bright fur |
| 1 | 0–2% | Easy to smear and loose stool, ≤1 cecotrophs | 0–30% | 0–30% | Dim fur |
| 2 | 2–5% | Loose stool, 2–3 cecotrophs | 30–60% | 30–60% | Shagged fur |
| 3 | 5–10% | Loose smeared stool in cage, 4–5 cecotrophs | 60–90% | 60–90% | Smudgy, unclean fur |
| 4 | >10% | Loose smeared stool in cage, > 5 cecotrophs | >90% | >90% | Smudgy, stool stains, smeared anus |

**Table 2** Primers for qPCR

| Marker | Forward primer Backward primer | Primer location within CDS | Target size | NCBI Accession |
|---|---|---|---|---|
| IL-12p35 | AAGGCCAGACAAACTCTAGAATTC<br>TTGGTTAACTCCAGTGGTAAACAGG | Exon 3/4 and 4/5 from ~8 | 116 nts | XM_002716291 |
| iNOS | GACGTCCAGCGCTACAATATCC<br>GATCTCTGTGACGGCCTGATCT | Undetermined | 102 nts | XM_002718780 |
| IFNγ | TGCCAGGACACACTAACCAGAG<br>TGTCACTCTCCTCTTTCCAATTCC | Exon 1 and 2/3 from 4 | 127 nts | NM_001081991 |
| GAPDH | TGACGACATCAAGAAGGTGGTG<br>GAAGGTGGAGGAGTGGGTGTC | Exon 1 of 1 | 120 nts | NM_001082253 |

modifications. Briefly, the dissected mucosa was washed with $Ca^{+}$- and $Mg^{+}$-free PBS; the caecal fold was removed and discarded. The tissue was cut and incubated in medium containing 20 mM EDTA (Sigma-Aldrich, St. Louis, MO, USA) for 30 min at 37°C on a shaking platform (150 rpm). After incubation, the suspension of IEC, villus cells, subepithelial cells and intestinal epithelial lymphocytes was detached by vortexing and passing through a 70-μm cell strainer (BD Biosciences, Erembodegem, Belgium). The epithelial cells were washed twice, pelleted, resuspended in RTL buffer (Qiagen), snap-frozen in liquid nitrogen and stored at −80°C for later analysis. The remaining tissue containing LP with muscle layer was collected and incubated in medium containing 1 μg/ml collagenase type I CLS (Worthington Biochemical Corp., Freehold, New Jersey, USA) at 37°C on a shaking plate (300 rpm). After 15 min incubation, the suspension was vortexed and filtered through a 70-μl strainer. The filtered cells were resuspended in 5% BSA in PBS to stop the enzymatic digestion. The undigested tissue was incubated with fresh collagenase solution for additional 15 min. The collagenase digestion was repeated three times, and the washed LPMC were pooled. LPC were pelleted twice and resuspended in DMEM supplemented with 5% FCS. LPMC were purified using Ficoll-Paque PLUS (GE Healthcare Europe GmbH, Freiburg Germany) gradient centrifugation for 40 min at 150×g. The viability of the cells was confirmed by tryptan blue staining. Cells were resuspended in RTL buffer (Qiagen), snap-frozen in liquid nitrogen and stored at −80°C for later analysis.

### *RNA isolation and genomewide mRNA expression analysis*

Total RNA was isolated with the Qiacube system using the RNeasy Mini Kit with DNase digestion (Qiagen) to eliminate genomic DNA. RNA integrity and quantity were determined on the Agilent 2100 Bioanalyzer (Agilent, Palo Alto, CA, USA). Samples with an integrity score ≥6.8 were sent to the Functional Genomic Centre Zurich (FGCZ) for sequencing on the Illumina® platform. The fold change (FC) was used to express the changes in average gene expression between studied groups. FC was normalized against the control group (rabbits receiving fennel tea only). The ENSEMBLE IDs were annotated using BetterBunny augmented annotation and analysis of rabbit genes (http://cptweb.cpt.wayne.edu) (Craig *et al.* 2012). MetaCore™ (Thomson Reuters, http://portal.genego.com) was used to perform network and pathway analyses. The following cut-offs were applied to select differentially expressed genes for further analysis: *P*-value $P \leq 0.01$ and fold change ≥|2.0|. The pathways (groups of genes belonging to the same pathway map in MetaCore™ database) and gene families were considered significant with a *P*-value ≤0.05 and were further selected on the basis of their relevance to inflammatory bowel disease pathology. Additional gene expression data sets for comparison were obtained from GEO Data Sets (NCBI) of previously published studies in colon pinch biopsies from patients with UC and CD (Granlund *et al.* 2013).

### *Validation of the genomewide mRNA expression analysis*

The expression profiling results were confirmed by qPCR of selected genes involved in the highlighted pathways. cDNA synthesis was performed using a High-capacity cDNA Reverse Transcription Kit (Life Technologies Ltd). Real-time PCR was performed using TaqMan Gene Expression Assays (Life Technologies Ltd) and TaqMan Fast Universal PCR Master Mix No AmpErase UNG (Life Technologies Ltd) on a 7900 HT Fast Real-Time PCR System with SDS 2.2 Software (Life Technologies Ltd). TaqMan gene expression assays were performed for COX-2 (Ptgs2, Oc03398293 _m1), IL-6 (Oc04097051_m1), MMP-1 (Oc04250656_m1)

**Table 3** Scoring system for DSS-induced histological changes in the caecum

| | Morphological features | | | Inflammation | | |
|---|---|---|---|---|---|---|
| | Villous stunting | Villous epithelial injury | Crypt distortion | Intraepithelial lymphocytes | LP lymphocytes and plasma cells | LP eosinophils |
| 1 | Normal mucosa | Normal mucosa | Normal mucosa | 5–10/50 IEL/epithelial cells | 25% of the villous lamina propria | 2–3 cells per × 40 field |
| 2 | Mild villous stunting | Mild villous epithelial injury | Mild crypt distension, hyperplasia and distortion | 11–30 IEL/50 epithelial cells. | 25–50% of the villous lamina propria | 5–10 per × 40 field. |
| 3 | Moderate villous stunting | Moderate villous epithelial injury | Moderate crypt distension, hyperplasia and distortion. | 31–50 IEL/50 epithelial cells may be focally clustered. | 50–75% of the villous lamina propria. | 10–20 per × 40 field. |
| 4 | Marked villous stunting | Marked villous epithelial injury | Marked crypt distension, hyperplasia and distortion | 51–100 IEL/50 epithelial cells, may be clustered and at all levels of the epithelium | 75–100% of the villous lamina propria. | > 20 per × 40 field |

and the housekeeping gene GAPDH (Oc03823402_g1) as an endogenous control. Measurements were performed in triplicates; relative expression was calculated using the ΔΔCt method.

### *Histopathological evaluation of colitis*

After careful dissection and fixation, tissues were routinely embedded in paraffin. Serial sections of 5 μm were cut using a microtome (Carl Zeiss AG, Feldbach, Switzerland) and stained with haematoxylin–eosin to investigate epithelial damage and cellular infiltration. The histological changes in the caecum were quantified in a blinded manner by two investigators with a scoring system (range 1–24) for morphological features and infiltration of immune cells according to the scoring system described in Table 3 (Cooper *et al.* 1993; Kojouharoff *et al.* 1997; Day *et al.* 2008).

### *Analysis of myeloperoxidase activity*

Myeloperoxidase (MPO) activity was measured in different regions of the gastrointestinal tract as previously described. Myeloperoxidase activity was calculated as mean absorbance (460 nm) per incubation time per protein content of

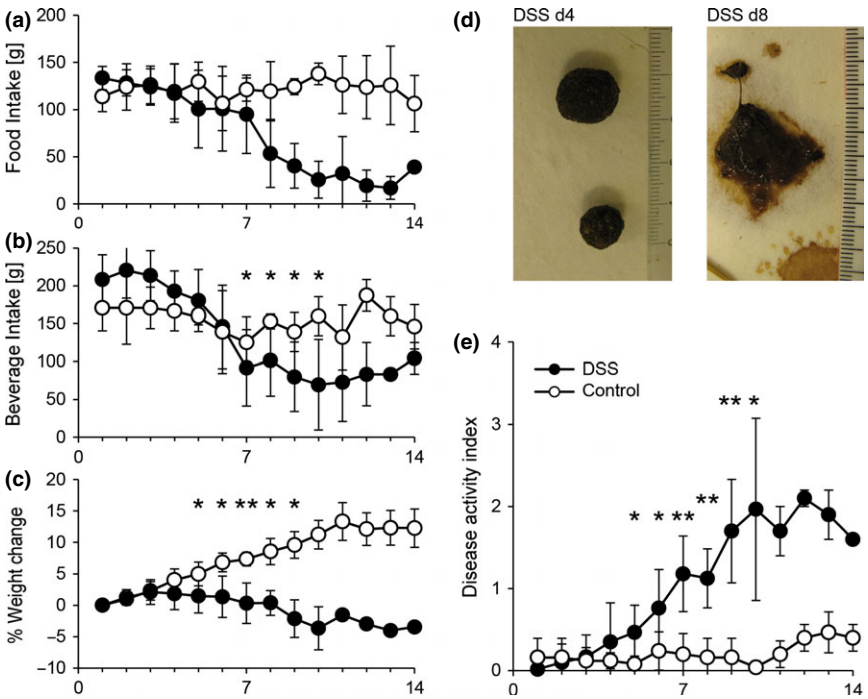


**Figure 1** Manifestation of clinical symptoms upon DSS exposure. Response to colitis induction was monitored daily according to a detailed score sheet. Food intake (a), beverage intake (b), weight change (c), stool consistency (d. representative pictures for control and DSS rabbits at day 10) were summarized into a disease activity index (e. DAI, 0–4). DSS rabbits (●, $n = 12$) were fed with 0.1% DSS in the daily beverage (fennel tea) for 5 days. The control group (○, $n = 5$) was maintained under the same conditions with fennel tea as beverage. Data represent mean ± SD; Mann–Whitney test, $^{**}P \leq 0.005$, $^{*}P \leq 0.05$.

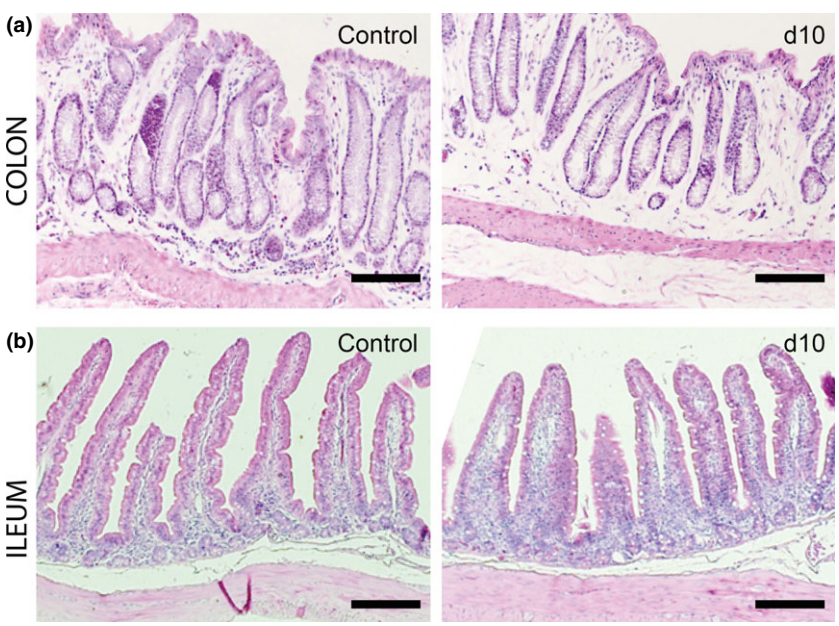


**Figure 2** Absence of histopathology in the colon and ileum. Representative HE-stained colon (a) and ileum (b) sections in control and in DSS-exposed rabbits at day 10. Scale: 200 μm.

the sample in grams (indicated as arbitrary units U/g s) (Bozeman *et al.* 1990).

### *Statistical analysis*

The results of the 0.1% DSS colitis were obtained in two different experiments ($n = 8$ and $n = 4$). As the experimental protocol was identical for both experiments, results were pooled together. The data obtained from this study were analysed using IBM SPSS statistic 21 (Armonk, NY, USA). The majority of the examined parameters were asymmetrically distributed. For the comparison of the treatment groups, the nonparametric Mann–Whitney *U*-test for two independent samples was used.

## Results

### *Clinical symptoms of DSS exposure in rabbits*

As rabbits have a more sensitive digestive tract in comparison with mice, the concentration of DSS to induce colitis had to be drastically decreased. We observed a reduction of daily fluid intake that we ascribed to the unpleasant taste of DSS. To overcome this problem, DSS was dissolved in organic fennel tea that successfully masked the taste of the DSS and restored a normal fluid intake during DSS exposure.

A pilot study (data not shown) showed that administration of 0.1% DSS in fennel tea for 3 days reduced the

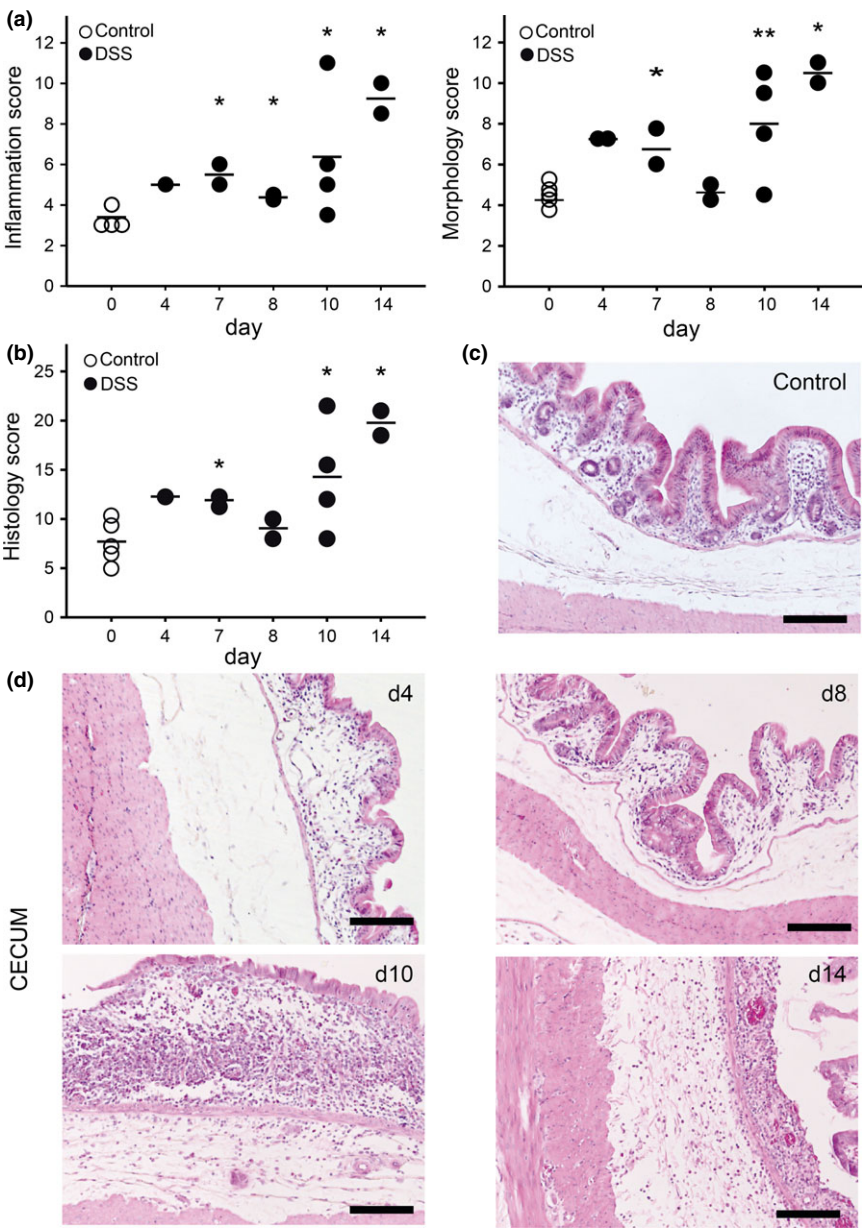


**Figure 3** Histopathological changes of the caecum at different time points after colitis induction. HE-stained caecum sections were scored (a, 1–4) for markers of inflammation (infiltration of lamina propria eosinophils, lamina propria lymphocytes, intraepithelial lymphocytes) and for the distortion of morphological features (villous stunting, villous epithelial injury, crypt distortion). Single parameters were summarized to a global score (b). Black dots represent DSS-treated rabbits (●); white dots represent control rabbits (○). Horizontal lines represent the arithmetical mean; Mann–Whitney test, $^{**}P \leq 0.05$, $^{*}P \leq 0.1$. Representative HE-stained caecal sections of control rabbits (c) and of DSS-exposed rabbits at different time points after colitis induction (d). Scale: 200 μm.

normal weight gain from day 5 on in the treated animals. This effect was no longer present from day 14 on, indicating a restitution of the colitis. Other clinical symptoms were not evident. Histological analysis of HE stained intestinal samples showed no clear signs of inflammation; only a slight reduction in the number of goblet cells in the caecum at day 7 and 10 was observed. Subsequently, the duration of the DSS phase was increased from 3 to 5 days. Twelve white Himalayan rabbits were fed for 5 days with 0.1% DSS in the daily beverage (fennel tea), whilst control rabbits ($n = 5$) housed in the same facility were given fennel tea without DSS. The earliest symptoms manifested at day 4, when the rabbits started to gradually diminish the daily food and beverage intake from the initial 120 g/day pellet and 210 ml/day beverage intake at day 1 down to 40 g/day and 100 ml/day at day 7 (Figure 1a, b).

Exposure to 0.1% DSS markedly reduced the weight gain (Figure 1c). Further symptoms included the presence of loose and smeared stool (Figure 1d), behavioural abnormalities such as apathy or aggressiveness and unclean fur. A combinatorial index of disease, (Figure 1e, disease activity index DAI, described in the methods section) was used to quantify the severity of the monitored clinical symptoms. We found that whilst the DAI of control rabbits remained

**Table 4** Genes concordantly upregulated in LPMC of DSS colitis rabbits and IBD biopsies

| | |
|---|---|
| Cell adhesion and cytoskeleton reorganization | Metabolism and biosynthesis |
| CD38 | PTGS2(COX2) |
| PLEK | SLC6A14[a] |
| S100A9 | TCN1 |
| SELL[a] | |
| Cytokine and cytokine R genes | Development |
| IL1A | EGR2[a] |
| IL6 | |
| IL8 | |
| IRF1 | |
| Chemokine and chemokine R genes | Tissue remodelling genes |
| CCR7[a] | MMP3 |
| CXCL10 | |
| CXCL11 | |
| CXCR4 | |
| ENA-78[a] | |
| Immune response | |
| *Innate immune defence* | *BCR and TCR signalling* |
| TMEM173 | CD19 |
| DMBT1 | LAX1 |
| FAM65B[a] | |
| SLC11A1[a] | |

List of genes concordantly upregulated in LPMC from the caecum of DSS-treated rabbit and colonic biopsies of inflamed tissue from patients with IBD. LPMC: Lamina propria mononuclear cells. [a]differentially expressed in patients with UC, only.

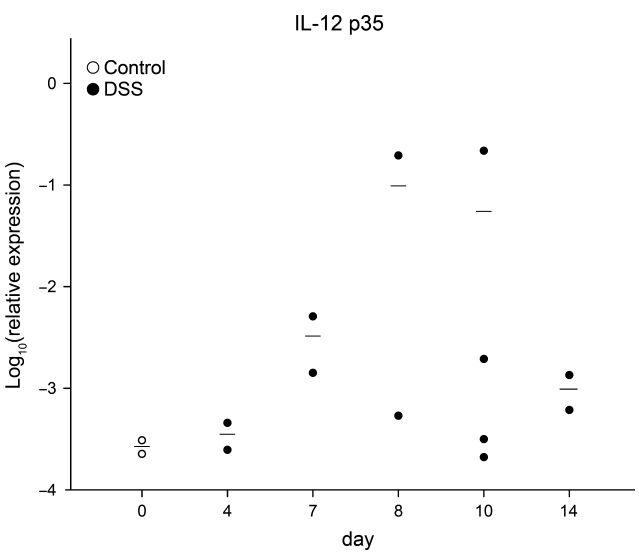


**Figure 4** mRNA expression of pro-inflammatory cytokines during colitis induction. mRNA expression of IL-12 p35 in caecum from DSS-treated (●) or control (○) rabbits. Results are shown as mean expression relative to GAPDH using the $2^{-\Delta\Delta Ct}$ method. Dots represent single rabbits; horizontal lines represent the arithmetical mean. Each sample was analysed in triplicate.

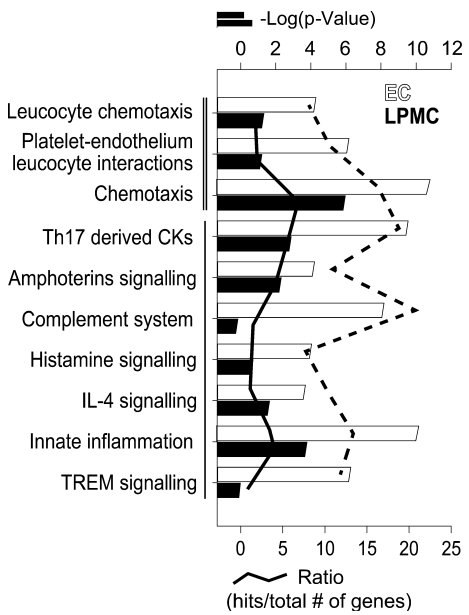


**Figure 5** Process network analysis of differentially expressed genes in epithelial cells (EC, black bars and line) and lamina propria mononuclear cells (LPMC, grey bars and line). This analysis is based on a manually curated database of process networks, which details more specific biological processes than GO annotations alone. Most prominent process networks associated with the identified genes were involved in cell adhesion and chemotaxis (═) and immune and immune responses (▬). Analysis was performed with MetaCore™. Bars represent the log(p-value) of enriched pathways, whereas lines represent the ratio between differentially expressed genes upon DSS exposure and the total number of genes involved in the specific process network. Gene expression threshold: fold change $\geq |2.0|$; $P$-value $\leq 0.05$.

at baseline (DAI <0.5), the DAI of rabbits receiving DSS increased significantly starting from day 5 (DSS: 0.47 ± 0.32, $n = 12$; control: 0.08 ± 0.10. $n = 5$) and rose up to 2.1 at day 12.

### *DSS induces a caecum-localized pathology*

Histological evaluation of the intestinal tract revealed a caecum-localized pathology, whereas no clear signs of tissue damage were observed in other regions of the intestinal tract (colon and ileum, Figure 2).

Histopathology of the caecum was characterized by infiltration of immune cells into the epithelial layer and the lamina propria and by morphological changes such as villous stunting, crypt distortion and villous epithelial injury (Figure 3a,c,d). The global histology score was increased from day 4 onward (Figure 3b). The severity of the damage increased progressively even after the removal of DSS from a baseline value of 7.7 ± 0.9 in control rabbits ($n = 5$) to an average score of 13.3 ± 5.0 at day 10 ($n = 4$) and further increased until day 14.

### *Expression analysis of genes involved in the immune response*

To evaluate the inflammatory response in DSS-treated rabbits, we analysed the mRNA expression of inflammation-related genes by q-rtPCR. iNOS, IFNγ and IL-12 p35 were chosen as they have been implicated in IBD and have been shown to be overexpressed in inflamed rabbit tissue (Schnupf & Sansonetti 2012). Gene expression analysis of inflammatory markers in the caecum showed a transient increase of IL-12 p35 in DSS-treated rabbits (Figure 4), although, owing to the limited sample number in the control group, the difference did not reach statistical significance. No difference between the groups was observed for iNOS and IFNγ.

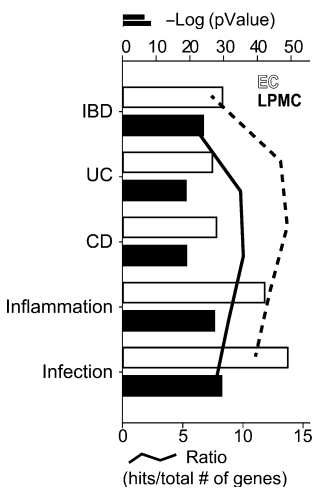


**Figure 6** Enrichment of differentially expressed genes in selected disease categories (by biomarkers) in epithelial cells (IEC, white bars and line) and lamina propria mononuclear cells (LPMC, grey bars and line). The Gene IDs of the orthologous genes assigned to the differentially expressed rabbit mRNAs were analysed for enrichment in selected disease categories using MetaCore™. Terms relevant for IBD and experimental colitis are displayed. Bars represent the log (*P*-values) of enriched pathways, whereas lines represent the ratio between the differentially regulated genes upon DSS exposure and the total number of genes involved in the specific process network. IBD, inflammatory bowel disease, UC, ulcerative colitis, CD, Crohn's disease. Gene expression threshold: fold change ≥ |2.0|; *P*-value ≤0.05.

### *Genomewide gene expression analysis in LPMC and IEC by RNAseq*

Genomewide gene expression analysis identified 470 differentially expressed genes in IEC and 215 differentially expressed genes in LPMC (FC ≥ |2|, $P \leq 0.05$). The process networks that were significantly over-represented in

**Table 5** Genes concordantly upregulated in ECs of DSS colitis rabbits and IBD biopsies

| | |
|---|---|
| Cell adhesion and cytoskeleton reorganization | Metabolism and biosynthesis |
| SELL[a] | FCRLA[b] |
| PLEK | PLA2G7[a] |
| VNN1 | SLC11A1[a] |
| S100A9 | SLC2A3 |
| CLEC4A | SLC6A14[a] |
| CD38 | TCN1 |
| Cytokine and cytokine R genes | Apoptosis |
| IL1A | UBD |
| IL1B | IER3[a] |
| IL6[a] | PEA15[a] |
| IL8 | |
| Chemokine and chemokine R genes | Cell–cell signalling |
| CCR7[a] | ADM |
| CXCL10 | TNFAIP6[a] |
| CXCL11 | **Tissue remodelling genes** |
| CXCL13 | CTSK |
| CXCL5[a] | MMP1 |
| CXCL6 | MMP12 |
| CXCL9 | SERPINE2 |
| Immune response | |
| *Innate immune defence* | *BCR and TCR signalling* |
| OAS2 | CD19 |
| TLR8[b] | CD74 |
| *Humoral immune response* | CD79B |
| POU2AF1 | CD86[a] |
| CD83[a] | LYN[a] |
| *Acute-phase response* | SLAMF8[a] |
| SERPINA1 | *Inflammatory response* |
| *Antigen processing* | NFKBIZ[a] |
| HLA-DMA | *Anti-inflammatory response* |
| HLA-DPA1 | A1F1 |
| HLA-DPB1[b] | |

List of genes concordantly upregulated in EC from the caecum of DSS-treated rabbit and colonic biopsies of inflamed tissue from patients with IBD. EC: epithelial cells. [a]genes differentially expressed in patients with UC, only. [b]genes differentially expressed in patients with CD, only.

the MetaCore™ analysis were 58 in LMPC and 49 in IEC respectively. Among the most relevant process networks, there was an over-representation of genes involved in inflammation, immune response and chemotaxis (Figure 5).

Furthermore, the disease (by biomarkers) ontology in MetaCore™ was used to assess the similarity between the gene expression in our rabbit DSS colitis model with the gene expression known to be associated with selected human diseases. In both LPMC and EC, we found an enrichment of differentially expressed genes associated with inflammation, IBD, CD and UC (Figure 6).

To further confirm the results of the disease enrichment analysis, we compared genes differentially regulated in our DSS colitis model with a gene set from a genomewide gene expression analysis in human CD and UC patients (Granlund *et al.* 2013). Overall, the majority of the differentially expressed genes were involved in immune response, cell adhesion, cytoskeleton reorganization and chemokine signalling (Table 4; Table 5).

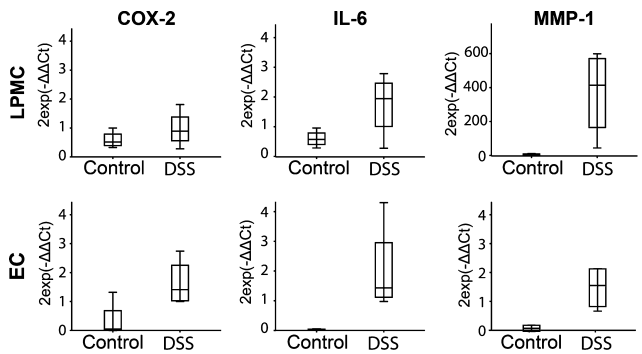


**Figure 7** Quantitative RT-PCR showing expression of COX-2 (a, d), IL-6 (b, e) and MMP-1 (c, f) in intestinal epithelial cells (IEC, upper panel) and lamina propria mononuclear cells (LPMC, lower panel) of DSS and control rabbits at day 10 postcolitis induction. Expression is shown relative to GAPDH in the distal colon, $n = 4–9$. Values are given as mean ± SD and difference between groups was tested by two-tailed Student's *t*-test.

Finally, the sequencing results for mRNA expression were validated for COX-2, IL-6 and MMP1 by qPCR (Figure 7). In accordance with our transcriptome results, the expression of the selected genes was higher in both LPMC and EC isolated from DSS-treated rabbits in comparison with the non-colitic controls.

### *DSS transiently increases neutrophil infiltration in the rabbit caecum*

The neutrophil infiltration into inflamed tissues was monitored by analysis of myeloperoxidase (MPO) activity (Bradley *et al.* 1982). MPO activity in the caecum of DSS-treated rabbits transiently increased at days 5–7 before returning to baseline levels at day 14 (Figure 8a), but due to the low number of animals the change did not reach statistical significance. Analysis of MPO in the ileum and the colon showed no significant differences between colitis animals and the control group (Figure 8b,c). In the ileum, the basal MPO activity in untreated rabbits was higher than in the caecum, but no changes occurred upon exposure to DSS. Overall, our results suggest that the DSS-induced infiltration of neutrophils predominantly localizes in the caecum.

## Discussion

The helminth parasite *T. suis* has shown promising results for the treatment of IBD in human studies. Unfortunately, efficacy and safety (in particular in immune-compromised subjects) as well as the underlying mechanisms cannot be studied in the well-established mouse and rat models of IBD as the parasite's ova fail to hatch in the intestine of these rodents. TSO are known to hatch in pigs (the natural host), humans and rabbits. As the life cycle of *T. suis* in humans and in rabbits appears similar, a rabbit model of colitis would represent an adequate model for investigations into TSO therapy. The aim of the present study was to develop an IBD model in rabbits by administration of DSS into the daily fluid intake. This study shows that adminis-

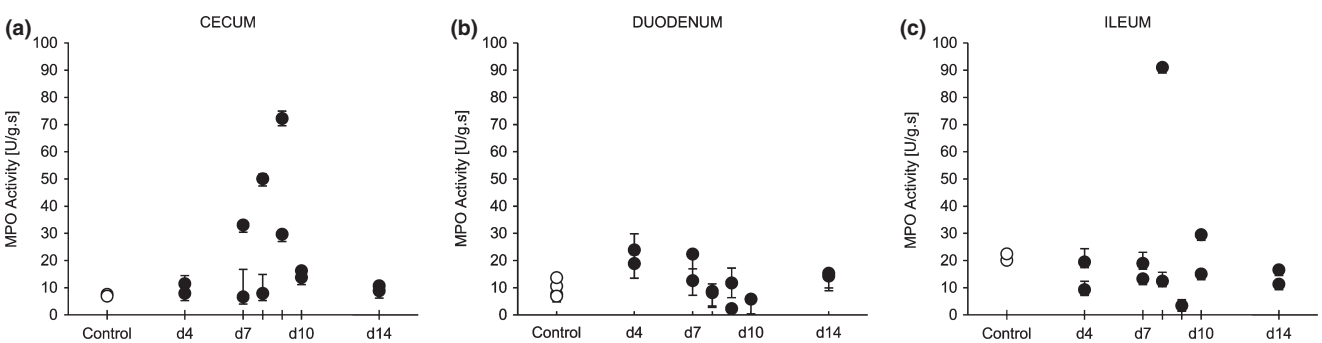


**Figure 8** Myeloperoxidase (MPO) was determined as a marker for neutrophil infiltration in the gastrointestinal epithelium. Values for MPO activity in caecum (a), duodenum (b) and ileum (c) samples were normalized for the total protein concentration as determined by BCA assay and for the incubation time (values are represented in arbitrary units U/g s). Dots represent single animals.

tration of 0.1% DSS for 5 days is sufficient to induce a clear acute inflammation that is localized in the caecum. Localization of the pathology in the caecum makes the DSS model particularly suitable to study the effects of TSO treatment as the caecum is the site of *T. suis* colonization in rabbits.

In accordance with the disease manifestation in other species, the clinical symptoms observed in rabbits were reduced weight gain, reduced food and beverage intake, loose stools and unclean fur (Wirtz *et al.* 2007). The strong reduction in fluid intake began after 5 days only; hence, the daily intake of DSS remained constant throughout the whole induction phase.

The reduction in food intake reflects the response to abdominal discomfort and the disturbances in feeding behaviour that are seen in patients with inflammation of the gastrointestinal tract (Rigaud *et al.* 1994) and are also commonly observed in mouse and rat models of gastrointestinal inflammation (McHugh *et al.* 1993; McDermott *et al.* 2006). To facilitate the evaluation of the disease outcome, we developed a DAI based on the monitoring of the different clinical parameters. Starting from day 4 after DSS administration, rabbits manifested clear symptoms of pathology that gradually worsened. A peak of disease activity was reached at day 9. Afterwards, the DAI decreased and stabilized until the last analysed time point at day 14.

Macroscopical analysis of the internal organs following euthanasia showed no abnormalities. In contrast, histopathological analysis of the intestinal tract revealed that DSS causes an inflammation predominantly localized in the caecum. The other sections of the large intestine and the small intestine remained unaffected.

The caecum localization of the DSS-induced inflammation is also observed in guinea pigs and in the Mongolian gerbil model (Iwanaga *et al.* 1994; Bleich *et al.* 2010). These species possess a functional caecum that is particularly enlarged and provides a niche for the microbial fermentation of cellulose (Snipes 1982, 1997). The caecum localization of the DSS-induced inflammation might be due to an increased permeability of the intestinal barrier to DSS in this particular section of the intestine (Hoshi *et al.* 1996). The localization of the lesions in gerbils has been linked to the increased absorption of sulphated polysaccharides in this particular section of the gerbil intestine, and absorption of DSS in the caecum has also been reported in rabbits (Sharratt *et al.* 1971) and might explain our observations. In accordance with DSS models in other species, DSS treatment induced both a disruption of the mucosal morphology and an infiltration of immune cells (Melgar *et al.* 2005). In particular, the histopathology of the caecum displays crypt loss, epithelial damage and infiltration of immune cells. These manifestations reproduce characteristic traits commonly observed in ulcerative colitis (Okayasu *et al.* 1990). Despite the progressive amelioration of the clinical symptoms after their peak at day 9, the histological damage persists longer and displays some characteristics of chronic intestinal inflammation such as the atypical branching of the crypts.

The initial pathology (day 4–9) presents classical features of an acute inflammation. From day 7 to day 10, we observed a transient increase in neutrophil infiltration into the caecal mucosa accompanied by an increased expression of the pro-inflammatory cytokine IL-12 p35. This transient inflammatory activity correlates well with the peak of the DAI and with the histological findings and suggests an initial T helper 1-driven acute response. The increased neutrophil activity in the caecal mucosa is a common feature with the guinea pig colitis model. However, the described model in guinea pigs was performed with high concentration of DSS (3%) and had a fulminant outcome, with 96% of the animals dying within 96 h (Iwanaga *et al.* 1994).

Genomewide mRNA expression profiling in caecum LPMC and ECs at day 10 showed an enrichment of genes involved in chemotaxis and immune response. In particular, the immune response was characterized by genes involved in Th17 signalling, particularly in epithelial cells. An activation of the innate immune response is a feature shared by both patients with CD and UC. In contrast, Th17-associated cytokines are usually observed in the inflamed mucosa of patients with CD, only. Our analysis further showed enrichment for IL-4-related cytokines that would rather suggest a Th2-type response. This type of response correlates well to the atypical Th2 response (mediated by natural killer cells producing IL-13) observed in patients with UC (Fuss *et al.* 2004). A switch into a Th2-type response has been observed as the colitis matures from an acute towards a chronic phase (Alex *et al.* 2009). The features that appear at later stages of the rabbit colitis might indicate that after an acute phase characterized by severe clinical symptoms, mucosal damage and acute inflammation, the pathology acquires a certain degree of chronicity with a shift towards a Th12 immune response. A long-term analysis is necessary to investigate these preliminary observations and to clarify whether the disease resolves after the acute phase or whether it progresses to chronicity.

In summary, we report the development and characterization of a novel DSS-induced colitis model in rabbits. The initial pathology has an acute nature and is characterized by specific clinical symptoms, histopathological changes and higher mRNA expression of inflammatory markers. Our model provides a safe and reliable induction of colitis in rabbits that is particularly suitable to study the effects and mechanisms of TSO treatment in IBD.

## Acknowledgements

Dr Falk Pharma funded this study and participated in the study conception. The Authors take responsibility for the integrity of the data and the accuracy of the analysis. All of the authors were involved in the development and critical revision of the manuscript, and decision to submit the manuscript for publication.

IL performed the animal experiments, collected and analysed the samples, performed the genetic analysis and drafted the manuscript. FN performed the animal experi-

ments and collected the samples. KA was involved in sample preparation. AC scored the histology specimens. BT and RG contributed to the conception of the study. GR contributed to the interpretation of data; study concept and design; critical revision of the manuscript for important intellectual content; study supervision. IFW contributed to the interpretation of data; statistical analysis; study concept and design; writing and revision of the manuscript; study supervision.

## References


Alex P., Zachos N.C., Nguyen T. *et al.* (2009) Distinct cytokine patterns identified from multiplex profiles of murine DSS and TNBS-induced colitis. *Inflamm. Bowel Dis.* **15**, 341–352.

Anthony D., Savage F., Sams V. & Boulos P. (1995) The characterization of a rabbit model of inflammatory bowel disease. *Int. J. Exp. Pathol.* **76**, 215–224.

Anthony R.M., Rutitzky L.I., Urban J.F. Jr, Stadecker M.J. & Gause W.C. (2007) Protective immune mechanisms in helminth infection. *Nat. Rev. Immunol.* **7**, 975–987.

Bleich E.M., Martin M., Bleich A. & Klos A. (2010) The Mongolian gerbil as a model for inflammatory bowel disease. *Int. J. Exp. Pathol.* **91**, 281–287.

Bozeman P.M., Learn D.B. & Thomas E.L. (1990) Assay of the human leukocyte enzymes myeloperoxidase and eosinophil peroxidase. *J. Immunol. Methods* **126**, 125–133.

Bradley P.P., Priebat D.A., Christensen R.D. & Rothstein G. (1982) Measurement of cutaneous inflammation: estimation of neutrophil content with an enzyme marker. *J. Invest. Dermatol.* **78**, 206–209.

Clayburgh D.R., Shen L. & Turner J.R. (2004) A porous defense: the leaky epithelial barrier in intestinal disease. *Lab. Invest.* **84**, 282–291.

Cooper H.S., Murthy S.N., Shah R.S. & Sedergran D.J. (1993) Clinicopathologic study of dextran sulfate sodium experimental murine colitis. *Lab. Invest.* **69**, 238–249.

Craig D.B., Kannan S. & Dombkowski A.A. (2012) Augmented annotation and orthologue analysis for Oryctolagus cuniculus: better Bunny. *BMC Bioinformatics* **13**, 84.

Day M.J., Bilzer T., Mansell J. *et al.* (2008) Histopathological standards for the diagnosis of gastrointestinal inflammation in endoscopic biopsy samples from the dog and cat: a report from the World Small Animal Veterinary Association Gastrointestinal Standardization Group. *J. Comp. Pathol.* **138**(Suppl 1), S1–S43.

Elliott D.E., Urban J.J., Argo C.K. & Weinstock J.V. (2000) Does the failure to acquire helminthic parasites predispose to Crohn's disease? *FASEB J.* **14**, 1848–1855.

Fuss I.J., Heller F., Boirivant M. *et al.* (2004) Nonclassical CD1d-restricted NK T cells that produce IL-13 characterize an atypical Th2 response in ulcerative colitis. *J. Clin. Invest.* **113**, 1490–1497.

Granlund A., Flatberg A., Ostvik A.E. *et al.* (2013) Whole genome gene expression meta-analysis of inflammatory bowel disease colon mucosa demonstrates lack of major differences between Crohn's disease and ulcerative colitis. *PLoS ONE* **8**, e56818.

Hathaway C.A., Appleyard C.B., Percy W.H. & Williams J.L. (1999) Experimental colitis increases blood-brain barrier permeability in rabbits. *Am. J. Physiol.* **276**, G1174–G1180.

Hodgson H.J., Potter B.J., Skinner J. & Jewell D.P. (1978) Immune-complex mediated colitis in rabbits. An experimental model. *Gut* **19**, 225–232.

Hoshi O., Iwanaga T. & Fujino M.A. (1996) Selective uptake of intraluminal dextran sulfate sodium and senna by macrophages in the cecal mucosa of the guinea pig. *J. Gastroenterol.* **31**, 189–198.

Hotta T., Yoshida N., Yoshikawa T., Sugino S. & Kondo M. (1986) Lipopolysaccharide-induced colitis in rabbits. *Res. Exp. Med. (Berl)* **186**, 61–69.

Iwanaga T., Hoshi O., Han H. & Fujita T. (1994) Morphological analysis of acute ulcerative colitis experimentally induced by dextran sulfate sodium in the guinea pig: some possible mechanisms of cecal ulceration. *J. Gastroenterol.* **29**, 430–438.

Knollmann F.D., Dietrich T., Bleckmann T. *et al.* (2002) Magnetic resonance imaging of inflammatory bowel disease: evaluation in a rabbit model. *J. Magn. Reson. Imaging* **15**, 165–173.

Kojouharoff G., Hans W., Obermeier F. *et al.* (1997) Neutralization of tumour necrosis factor (TNF) but not of IL-1 reduces inflammation in chronic dextran sulphate sodium-induced colitis in mice. *Clin. Exp. Immunol.* **107**, 353–358.

McDermott J.R., Leslie F.C., D'Amato M., Thompson D.G., Grencis R.K. & McLaughlin J.T. (2006) Immune control of food intake: enteroendocrine cells are regulated by CD4 + T lymphocytes during small intestinal inflammation. *Gut* **55**, 492–497.

McHugh K.J., Weingarten H.P., Keenan C., Wallace J.L. & Collins S.M. (1993) On the suppression of food intake in experimental models of colitis in the rat. *Am. J. Physiol.* **264**, R871–R876.

Melgar S., Karlsson A. & Michaelsson E. (2005) Acute colitis induced by dextran sulfate sodium progresses to chronicity in C57BL/6 but not in BALB/c mice: correlation between symptoms and inflammation. *Am. J. Physiol. Gastrointest. Liver Physiol.* **288**, G1328–G1338.

Melgar S., Karlsson L., Rehnstrom E. *et al.* (2008) Validation of murine dextran sulfate sodium-induced colitis using four therapeutic agents for human inflammatory bowel disease. *Int. Immunopharmacol.* **8**, 836–844.

Mennigen R., Nolte K., Rijcken E. *et al.* (2009) Probiotic mixture VSL#3 protects the epithelial barrier by maintaining tight junction protein expression and preventing apoptosis in a murine model of colitis. *Am. J. Physiol. Gastrointest. Liver Physiol.* **296**, G1140–G1149.

Mizoguchi A. (2012) Animal models of inflammatory bowel disease. *Prog. Mol. Biol. Transl. Sci.* **105**, 263–320.

Molodecky N.A., Soon I.S., Rabi D.M. *et al.* (2012) Increasing incidence and prevalence of the inflammatory bowel diseases with time, based on systematic review. *Gastroenterology* **142**, 46–54 e42; quiz e30.

Murthy S.N. (2006) Animal models of inflammatory bowel disease. In: *In Vivo Models of Inflammation*, pp. 137–174 (eds C.C. Stevenson, L.A. Marshall, D.W. Morgan), Basel: Birkhäuser.

Nell S., Suerbaum S. & Josenhans C. (2010) The impact of the microbiota on the pathogenesis of IBD: lessons from mouse infection models. *Nat. Rev. Microbiol.* **8**, 564–577.

Okayasu I., Hatakeyama S., Yamada M., Ohkusa T., Inagaki Y. & Nakaya R. (1990) A novel method in the induction of reliable experimental acute and chronic ulcerative colitis in mice. *Gastroenterology* **98**, 694–702.

Poritz L.S., Garver K.I., Green C., Fitzpatrick L., Ruggiero F. & Koltun W.A. (2007) Loss of the tight junction protein ZO-1 in dextran sulfate sodium induced colitis. *J. Surg. Res.* **140**, 12–19.

Rigaud D., Angel L.A., Cerf M. *et al.* (1994) Mechanisms of decreased food intake during weight loss in adult Crohn's disease

patients without obvious malabsorption. *Am. J. Clin. Nutr.* **60**, 775–781.

Rook G.A. (2011) Hygiene and other early childhood influences on the subsequent function of the immune system. *Dig. Dis.* **29**, 144–153.

Schnupf P. & Sansonetti P.J. (2012) Quantitative RT-PCR profiling of the rabbit immune response: assessment of acute Shigella flexneri infection. *PLoS ONE* **7**, e36446.

Scholmerich J. (2013) Trichuris suis ova in inflammatory bowel disease. *Dig. Dis.* **31**, 391–395.

Schwartz L., Abolhassani M., Pooya M. *et al.* (2008) Hyperosmotic stress contributes to mouse colonic inflammation through the methylation of protein phosphatase 2A. *Am. J. Physiol. Gastrointest. Liver Physiol.* **295**, G934–G941.

Sharratt M., Grasso P., Carpanini F. & Gangolli S.D. (1971) Carrageenan ulceration as a model for human ulcerative colitis. *Lancet* **1**, 192–193.

Snipes R.L. (1982) Anatomy of the guinea-pig cecum. *Anat. Embryol. (Berl)* **165**, 97–111.

Snipes R.L. (1997) Intestinal absorptive surface in mammals of different sizes. *Adv. Anat. Embryol. Cell Biol.* **138**, III–VIII, 1–90.

Strachan D.P. (1989) Hay fever, hygiene, and household size. *BMJ* **299**, 1259–1260.

Summers R.W., Elliott D.E., Qadir K., Urban J.F. Jr, Thompson R. & Weinstock J.V. (2003) Trichuris suis seems to be safe and possibly effective in the treatment of inflammatory bowel disease. *Am. J. Gastroenterol.* **98**, 2034–2041.

Watt J. & Marcus R. (1970) Ulcerative colitis in rabbits fed with degraded carrageenan. *J. Pathol.* **100**, 130–131.

Weigmann B., Tubbe I., Seidel D., Nicolaev A., Becker C. & Neurath M.F. (2007) Isolation and subsequent analysis of murine lamina propria mononuclear cells from colonic tissue. *Nat. Protoc.* **2**, 2307–2311.

Weinstock J.V., Summers R.W., Elliott D.E., Qadir K., Urban J.F. Jr & Thompson R. (2002) The possible link between de-worming and the emergence of immunological disease. *J. Lab. Clin. Med.* **139**, 334–338.

Wirtz S. & Neurath M.F. (2000) Animal models of intestinal inflammation: new insights into the molecular pathogenesis and immunotherapy of inflammatory bowel disease. *Int. J. Colorectal Dis.* **15**, 144–160.

Wirtz S., Neufert C., Weigmann B. & Neurath M.F. (2007) Chemically induced mouse models of intestinal inflammation. *Nat. Protoc.* **2**, 541–546.

Yan Y., Kolachala V., Dalmasso G. *et al.* (2009) Temporal and spatial analysis of clinical and molecular parameters in dextran sodium sulfate induced colitis. *PLoS ONE* **4**, e6073.